THE ASTRONOMICAL JOURNAL, 116:2965–2974, 1998 December

A Brγ PROBE OF DISK ACCRETION IN T TAURI STARS AND EMBEDDED YOUNG STELLAR OBJECTS

JAMES MUZEROLLE,[1,2] LEE HARTMANN,[2] AND NURIA CALVET[3]
Harvard-Smithsonian Center for Astrophysics, Mail Stop 42, 60 Garden Street, Cambridge, MA 02138; jmuze@cfa.harvard.edu, hartmann@cfa.harvard.edu, ncalvet@cfa.harvard.edu
Received 1998 May 15; revised 1998 July 2

ABSTRACT

We report on observations of Paβ and Brγ for a sample of classical T Tauri stars in Taurus and find a tight correlation between the emission-line luminosities and the accretion luminosity as measured from the hot continuum excess. We use the Brγ luminosity correlation to calculate accretion luminosities in highly reddened young stars with existing line measurements. The distribution of accretion luminosities is similar in Taurus and Ophiuchus Class II sources. For the deeply embedded Class I objects, the accretion luminosities are in general less than the bolometric luminosities, which implies that the disk accretion rates are significantly lower than the envelope infall rates. We find that the central sources of many Class I objects are quite similar to their Class II counterparts.

Key words: stars: pre–main-sequence — techniques: spectroscopic

1. INTRODUCTION

The mass accretion rate is an essential parameter in studying pre–main-sequence stellar evolution. As a function of time, the accretion rate traces the accretion of circumstellar material onto a young stellar object and can be used to constrain models of disk evolution (Hartmann et al. 1998, hereafter HCGD). Previous studies (Bertout, Basri, & Bouvier 1988; Basri & Bertout 1989; Hartigan et al. 1991; Valenti, Basri, & Johns 1993; Hartigan, Edwards, & Ghandour 1995; Gullbring et al. 1998, hereafter GHBC) have estimated the accretion rate for classical T Tauri stars (CTTS) in Taurus, with varying methods and assumptions.

The most obvious tracer of the accretion rate is the infrared-excess continuum emission caused by viscous dissipation in the disk. However, disk reprocessing of the incident stellar radiation also results in an infrared excess and cannot be easily disentangled from the accretion excess, especially at low and moderate accretion rates (Kenyon & Hartmann 1987). The most reliable accretion rate estimates have been determined by measuring the *blue* continuum excess emission observed in CTTS. This excess was originally thought to be emission from a boundary layer between the accretion disk and the central star (Bertout et al. 1988; Basri & Bertout 1989), although more recent investigations have supported a magnetospheric accretion scenario where the blue excess is emitted by an accretion shock where disk material infalling along magnetic field lines impacts the stellar surface (Calvet & Hartmann 1992; Edwards et al. 1994; Hartmann, Hewett, & Calvet 1994; Muzerolle, Calvet, & Hartmann 1998a; Calvet & Gullbring 1998). In either case, the hot continuum excess is a result of the energy of the accreting material and should therefore be a direct measure of the accretion rate. GHBC carefully measured accretion luminosities in CTTS using extracted blue excess spectra; in the process, they obtained the stellar properties (mass and radius) and thus derived accretion rates. They also found that accretion luminosities could be determined from U-band photometry, providing a more easily obtainable diagnostic.

However, measurements of the blue excess are possible only for stars with relatively low extinction. Some other tracer of the accretion luminosity/rate that is less affected by extinction is necessary for studying heavily reddened sources. We have begun to investigate emission-line diagnostics of accretion in CTTS. Radiative transfer models, in combination with high-resolution spectra, have shown that the broad permitted emission lines exhibited by CTTS are formed in the infalling magnetospheric flow (Hartmann et al. 1994; Muzerolle et al. 1998a; Muzerolle, Hartmann, & Calvet 1998b). Thus, one would expect the line strengths to depend on the accretion rate; we have discovered that this is the case for the Ca II infrared triplet (Muzerolle et al. 1998b). To study heavily reddened objects, we need to consider emission lines at even longer wavelengths so that the line fluxes are not as dependent on the (typically uncertain) extinction measurements. In this paper, we investigate the Paβ and Brγ emission lines in CTTS for this purpose.

Of special interest are the Class I, or embedded, objects. (There is considerable ambiguity and confusion in the literature with the terminology associated with highly extincted TTS and Class I sources. For clarity, we hereafter refer *only* to Class I objects—young stars with infalling envelopes—as being *embedded*.) Quantitative measurements of inner disk accretion in Class I objects are crucial to understanding the earliest stages of star formation and disk evolution. There are several major questions that have yet to be addressed satisfactorily, including the nature of the central source and the fraction of the final stellar mass that is accreted during the embedded phase. One important issue is the luminosity problem first reported by Kenyon et al. (1990). One can roughly estimate an accretion rate from infall (Kenyon et al. 1990). In Taurus, the typical age of an embedded source has been estimated to be $\sim 10^5$ yr (Myers et al. 1987; Kenyon et al. 1990), whereas the TTS population is $\sim 10^6$ yr. In order to build a typical mass (0.5 $M_\odot$) TTS, the time-averaged accretion rate for embedded stars is then $\sim 5 \times 10^{-6}$ $M_\odot$ yr^{-1}. This estimate is further supported by spectral energy distribution fitting of infall models (Kenyon, Calvet, &

[1] Also Five College Astronomy Department, University of Massachusetts, Amherst, MA.
[2] Visiting Astronomer, Kitt Peak National Observatory, operated by the National Optical Astronomy Observatory under contract to the National Science Foundation.
[3] Also Centro de Investigaciones de Astronomia, Mérida, Venezuela.

TABLE 1

STELLAR PARAMETERS

Object	Spectral Type	A_V	J	K	$\log L_{acc}/L_{\odot}$	$\log \dot{M}(M_{\odot}\ yr^{-1})$	Method
AA Tau	K7	0.74	9.42	8.00	−1.60	−8.48	b
BP Tau	K7	0.51	9.14	7.97	−0.75	−7.54	b
CY Tau	M1	0.32	9.74	8.49	−1.34	−8.12	b
DE Tau	M2	0.62	9.26	7.83	−1.15	−7.58	b
DF Tau	M0.5	0.45	8.28	6.82	−0.45	−6.91	b
DG Tau........	K7–M0	2.20	8.97	6.74	0.70	−6.10	b
DK Tau........	K7	1.42	8.88	6.99	−0.78	−7.42	b
DL Tau	K7	2.10	9.73	7.97	−0.22	−7.00	b
DN Tau........	M0	0.25	9.16	8.00	−1.80	−8.46	b
DO Tau........	M0	2.27	9.48	7.44	−0.22	−6.84	b
DR Tau	K7	1.60	8.95	6.80	0.44	−6.3	b
DS Tau	K5	0.34	9.59	8.28	−0.68	−7.89	b
GG Tau........	K7	0.60	8.78	7.34	−1.08	−7.76	b
GI Tau	K6	1.34	9.42	7.79	−1.03	−8.02	b
GK Tau........	K7	0.94	9.02	7.31	−1.46	−8.19	b
GM Aur	K7	0.31	9.37	8.48	−1.15	−8.02	b
HN Tau........	K5	0.65	10.82	8.44	−1.46	−8.89	b
IP Tau	M0	0.32	9.91	8.54	−2.15	−9.10	b
UY Aur	K7	1.26	8.63	6.87	−0.57	−7.18	b
CI Tau	K7	1.77	9.61	7.82	−0.36	−7.19	U
DH Tau........	M1	1.25	9.67	8.20	−1.54	−8.30	U
DP Tau	M0.5	1.46	10.33	8.37	−0.98	−7.88	U
FM Tau	M0	0.69	10.35	8.67	−1.36	−8.45	U
FQ Tau	M2	1.87	10.61	9.47	0.34	−6.45	U
FS Tau.........	M1	1.84	10.66	7.74	−1.13	−8.09	U
FV Tau	K5	4.72	9.51	7.37	0.75	−6.23	U
FX Tau	M1	1.08	9.16	8.14	−2.00	−8.65	U
GH Tau........	M2	0.52	9.22	7.78	−1.32	−7.92	U
Haro 6-37......	K6	2.12	9.31	7.40	−0.10	−7.00	U
IQ Tau.........	M0.5	1.25	9.74	8.10	−0.90	−7.55	U

NOTE.—Method denotes the procedure used to determine the extinctions, accretion luminosities, and mass accretion rates: b, blue spectrum analysis from GHBC and Calvet & Gullbring 1998; U, photometric calibration of U-band excess using mean magnitudes and extinctions from KH. J and K mean magnitudes also from KH.

Hartmann 1993a) and is consistent with the theoretical predictions of collapse for conditions in the Taurus-Auriga molecular cloud (Adams, Lada, & Shu 1987). The equivalent accretion luminosity ($L_{acc} = GM_* \dot{M}/R_*$), using a value for M_*/R_* assuming the typical embedded source lies on the birth line, is $\sim 20\ L_{\odot}$, which is an order of magnitude greater than the typical observed luminosity $L \sim 1\ L_{\odot}$. Thus, there is a large discrepancy between the expected accretion luminosity from infall and the maximum observed luminosity, implying that the stellar accretion rate (if $L = L_{acc}$) is less than the envelope infall rate. Kenyon et al. (1990) suggested that a likely solution to the luminosity problem is that the mass infall rate does not actually measure the rate of accretion onto the central protostar, but rather the rate of accretion onto the disk. Material must then accumulate in the disk until instabilities produce episodic FU Orionis outbursts with $\dot{M} \sim 10^{-4}\ M_{\odot}\ yr^{-1}$. The assumption that $L = L_{acc}$ is far from certain, however; independent estimates of the disk accretion rate and luminosity in Class I objects are essential.

There are two main goals of this paper: (1) to establish a calibration of infrared emission-line luminosity tracers of the accretion luminosity, and (2) to use the calibration to determine disk accretion luminosities in heavily extincted objects (including CTTS in ρ Ophiuchi and Class I objects in ρ Oph and Taurus) for the first time. Comparing observed line luminosities with previously determined accretion luminosities in a sample of Taurus CTTS, we find an excellent correlation for Paβ and Brγ. We then use the calibration to estimate accretion luminosities in highly reddened objects with previously published Brγ line luminosities and discuss the implications for accretion in the earliest stages of star formation.

2. OBSERVATIONS AND DATA REDUCTION

In order to calibrate a possible line luminosity versus accretion luminosity correlation, we chose a sample of Taurus CTTS for which the accretion rate has already been measured. The sample includes 19 stars with accretion rates determined by GHBC from their observations of the blue excess spectra and an additional 11 stars with accretion rates measured from the U-band excess (HCGD). Table 1 lists the sample objects, along with their extant infrared magnitudes, extinctions, and accretion rates. We also observed two weak-lined T Tauri stars (WTTS) in order to compare the behavior of the lines between accreting and nonaccreting systems. Observations were done with the infrared Cryogenic Spectrometer (CRSP) on the 2.1 m telescope at KPNO on 1998 January 9–12. We observed both Paβ and Brγ for each object, with wavelength ranges 1.22–1.32 and 2.08–2.22 μm, centered on each line, respectively. The resolution of the spectra is $R \sim 800$. We show some representative spectra in Figure 1.

The spectra were reduced using the standard IRAF routines.[4] Each object was observed at each line in two pairs of offset positions; the offset pairs were subsequently differenced (after flat-fielding) to remove background tellu-

[4] IRAF is distributed by the National Optical Astronomy Observatories, which is operated by the Association of Universities for Research in Astronomy, Inc., under contract to the National Science Foundation.

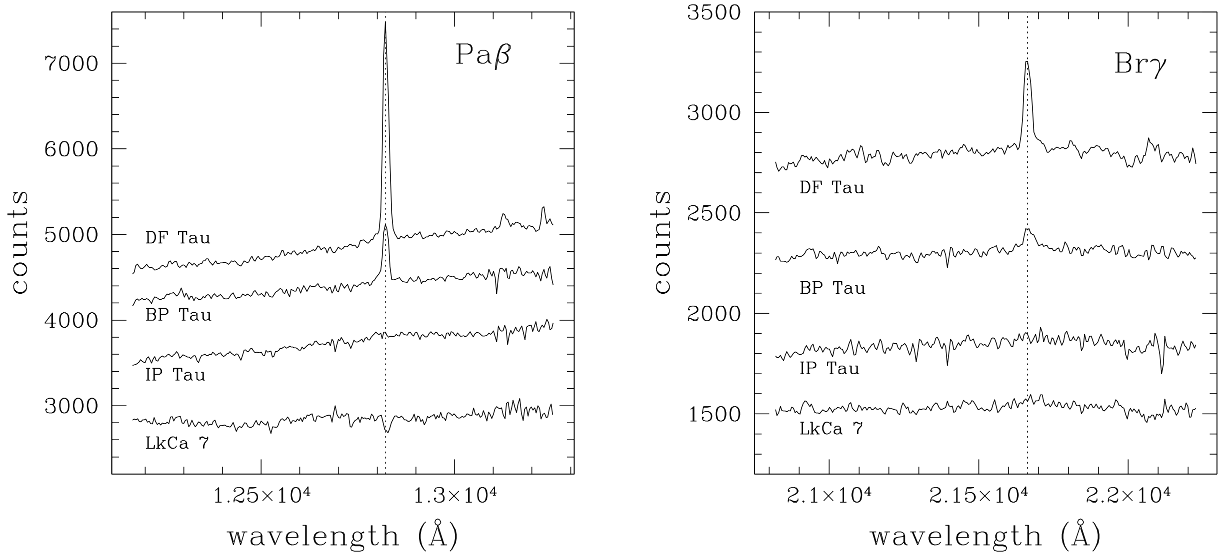

FIG. 1.—Paβ and Brγ spectra for three CTTS (spanning a range of accretion rates) and one WTTS (LkCa 7). The Paβ spectrum of LkCa 7 and the Brγ spectrum of IP Tau have been shifted down by 1500 and 700 counts, respectively, for clarity. All the spectra have been corrected for telluric absorption (see text).

ric emission lines. Each differenced spectrum was then wavelength calibrated using comparison lamp spectra, with an accuracy of about 1 Å (the Brγ calibration was slightly less accurate because of the smaller number of identifiable comparison lamp lines). Finally, the spectra were divided by telluric standard star spectra (of approximately the same air mass and time) in order to remove telluric absorption features. This proved to be somewhat problematic in that the usual hot star standards, preferable because of their relatively featureless spectra, have very deep hydrogen absorption lines. Thus, in addition to the hot star standards, we elected to observe later type (late-G and early-K) dwarf stars, which have far less Paβ absorption and virtually no Brγ absorption. Although the spectra of these standards are not featureless and contain many photospheric absorption features that will contaminate the division, we are primarily interested in only the hydrogen emission lines themselves. Thus, the rest of the observed spectrum is effectively sacrificed using late-type stars for telluric division. Before dividing into each object spectrum, we manually removed the Paβ absorption from the standard spectra by interpolating across the continuum to either side of the line. This may leave any telluric absorption near the line uncorrected. As a check, we compared the standard spectra as a function of air mass and saw no obvious feature growing in strength more than about 5% of the hydrogen absorption line.

3. CALIBRATION

The measured equivalent widths of Paβ and Brγ are shown in Table 2. Typical measurement errors are about 0.3 Å, as estimated by repeated measurements of each line. A few of the CTTS, including IP Tau and DN Tau, exhibit weak Paβ emission that only partially fills in the photospheric absorption (see Fig. 1). To measure the total emission, we subtracted the spectrum of a WTTS, which exhibits no Paβ emission, in order to remove the photospheric absorption feature. We used two different template stars, LkCa 7 and V819 Tau (both with spectral type K7, the typical spectral type of our sample), and got similar results. Lower limits indicate the lack of measurable emission in excess of the WTTS template. All but one of the CTTS in the sample, which by definition are actively accreting, show Paβ in emission; most (26/30) show Brγ in emission.

The CTTS sample was drawn from stars with known accretion rates, determined from either blue excess spectrophotometry (GHBC; Calvet & Gullbring 1998) or U-band photometry (HCGD). Table 1 indicates these two groups. Figure 2 shows the Paβ and Brγ equivalent widths plotted as a function of the accretion rate. A general trend of increasing equivalent width with increasing accretion rate can be seen, although there is considerable scatter.

The equivalent width is not a straightforward diagnostic since it is not a measure of the line strength alone but also depends on the continuum. Thus, we estimated the line *flux* using our measured equivalent widths, extinctions from GHBC and HCGD, and mean photometric magnitudes (J for the Paβ continuum, K for the Brγ continuum) from Kenyon & Hartmann (1995, hereafter KH). The line fluxes for both Paβ and Brγ are extremely well correlated with the

TABLE 2

EMISSION-LINE EQUIVALENT WIDTHS

Object	Paβ	Brγ	Object	Paβ	Brγ
AA Tau	3.2	1.7	GM Aur	14.2	7.4
BP Tau	3.0	2.2	HN Tau........	10.9	3.0
CY Tau	3.1	2.3	IP Tau	0.7	<0.3
DE Tau	4.2	2.0	UY Aur	3.5	1.5
DF Tau	9.6	4.9	CI Tau	7.0	4.2
DG Tau......	19.1	14.1	DH Tau........	1.0	0.5
DK Tau......	4.6	1.8	DP Tau	7.5	3.4
DL Tau	26.2	14.6	FM Tau	0.7	<0.3
DN Tau......	1.1	0.5	FQ Tau	0.9	<0.3
DO Tau......	15.4	6.1	FS Tau.........	6.5	2.6
DR Tau	21.2	7.3	FV Tau	4.5	1.0
DS Tau	4.8	2.5	FX Tau	2.0	1.4
GG Tau......	5.4	2.8	GH Tau........	<0.3	<0.3
GI Tau	1.5	1.5	Haro 6-37......	5.3	2.2
GK Tau......	1.7	0.7	IQ Tau.........	2.5	1.1

NOTE.—Equivalent widths given as negative values in angstroms.

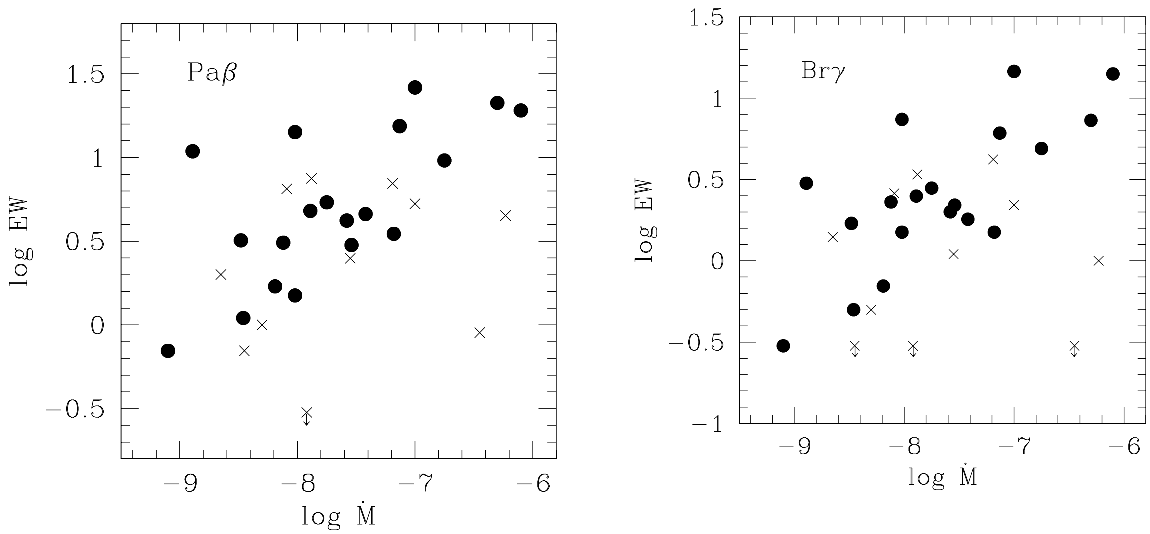

FIG. 2.—Emission-line equivalent widths in angstroms as a function of accretion rate. *Filled circles*, accretion rates from blue excess spectra; *crosses*, accretion rates from *U*-band photometry.

accretion rate (Fig. 3). We note that the typical dispersions in the *J* and *K* magnitudes are ~0.1–0.2 mag (KH), suggesting that time variability of the continuum will not affect our flux estimates substantially. Overplotted are results from our magnetospheric accretion models (see Muzerolle et al. 1998a). Using the same parameters as those that matched the Balmer emission lines, the model line fluxes can account for the observed infrared line emission, supporting our contention that these lines are produced in magnetospheres.

In Figure 3, we distinguish between the stars with $\dot{M}$ determined from spectrophotometry and the stars with $\dot{M}$ determined from *U*-band photometry. We expect the spectrophotometry to yield more accurate accretion rates since the data are simultaneous and the extinctions are estimated directly from the spectra, whereas the *U* excesses are calculated from mean *U* magnitudes and extinctions estimated from mean $V-R$ colors (neglecting the effects of veiling). The correlation is much tighter when one considers only the stars with spectrophotometric accretion rates. Two stars are markedly off the trend, FQ Tau and FV Tau. The extinctions, extremely important in determining dereddened *U* magnitudes and thus blue excesses, are highly uncertain for these stars (and in the case of FV Tau, extremely large). The A_V derived for FQ Tau from its $V-R$ color (used in HGCD) is much larger than that listed in KH (3.35 and 1.87, respectively). Thus, the line fluxes and accretion luminosities, both dependent on the extinction, should be called into question for these stars.

We next make a more direct comparison of line and accretion luminosities. The accretion luminosity (L_{acc}) is more straightforward than the accretion rate since one does not need to know a priori the stellar mass and radius. GHBC found a good correlation between the *U*-band luminosity and the accretion luminosity, which formed the basis for deriving $\dot{M}$ from *U*-band photometry. Figure 4 shows an

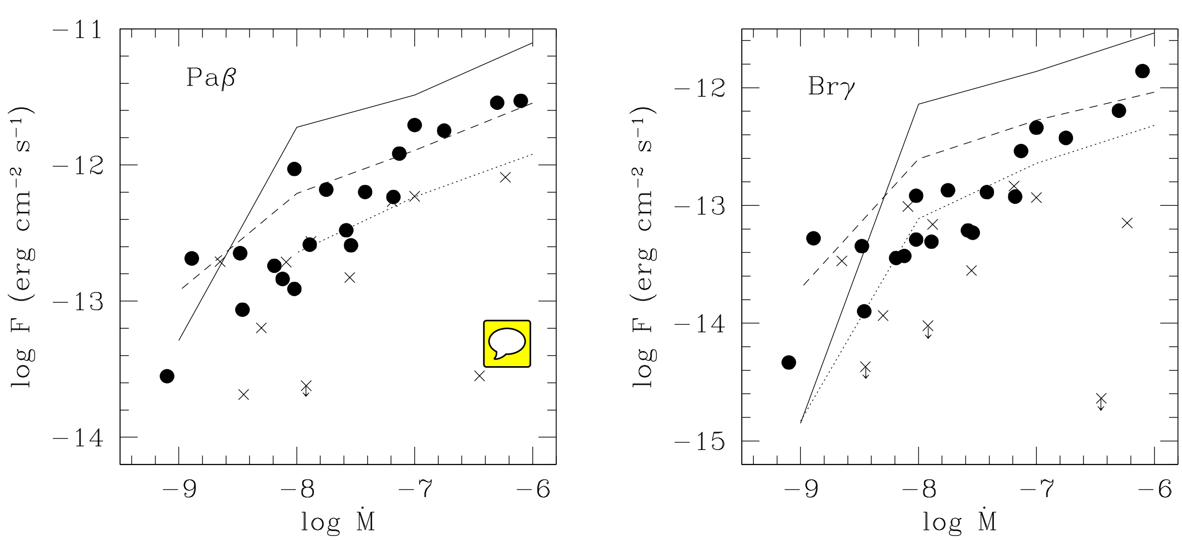

FIG. 3.—Emission-line fluxes as a function of accretion rate. *Filled circles*, accretion rates from blue excess spectra; *crosses*, accretion rates from *U*-band photometry. Lines represent emission-line fluxes from magnetospheric accretion models (see Muzerolle et al. 1998a): *dotted line*, $2.2 < R_{mag}/R_* < 3$ and $T_{max} = 8000$ K; *dashed line*, $2.2 < R_{mag}/R_* < 3$ and $T_{max} = 10{,}000$ K; *solid line*, $4 < R_{mag}/R_* < 6$ and $T_{max} = 10{,}000$ K.

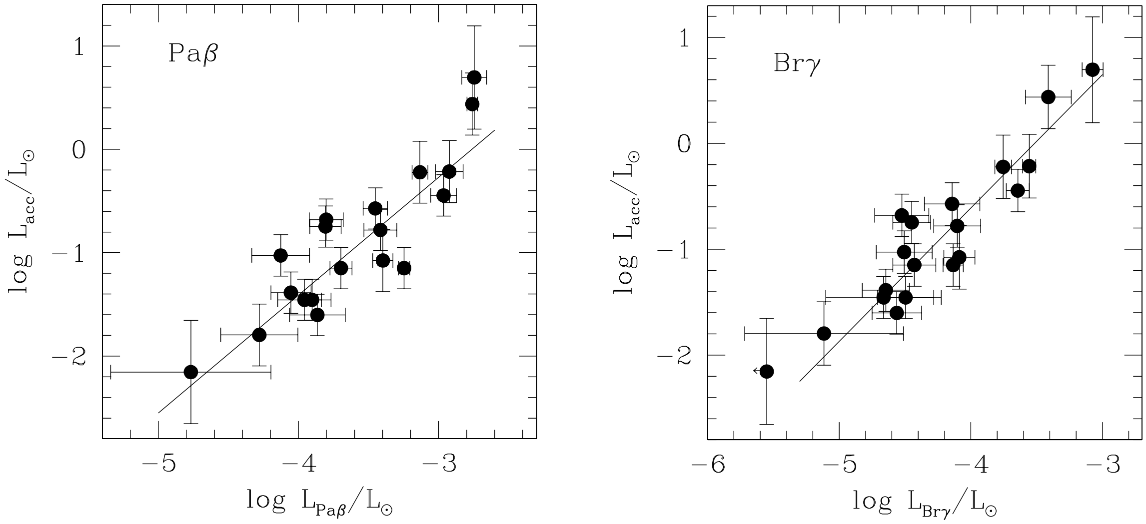

FIG. 4.—Correlation between the accretion luminosity and line luminosities. See text for discussion of error estimates.

analogous plot of L_{acc} versus the Paβ and Brγ line luminosities (here we use only the spectrophotometric data). Again, there is an excellent correlation, indicating that a measurement of the line luminosity directly measures L_{acc}. Once the stellar parameters, M_* and R_*, are known, $\dot{M}$ can then be calculated. From a least-squares fit of the data, taking into account estimated errors in both dimensions, we get

$$\log (L_{acc}/L_{\odot}) = (1.14 \pm 0.16) \log (L_{Pa\beta}/L_{\odot}) + (3.15 \pm 0.58) , \tag{1}$$

$$\log (L_{acc}/L_{\odot}) = (1.26 \pm 0.19) \log (L_{Br\gamma}/L_{\odot}) + (4.43 \pm 0.79) . \tag{2}$$

Errors for the accretion luminosity were taken to be about 0.2 dex typically (up to 0.5 dex for the low-luminosity stars like IP Tau), and errors for the line luminosities were estimated from our measurement uncertainties and the scatter in the J and K magnitudes used to compute the mean magnitudes in KH.

The lack of simultaneity between our observations and the spectrophotometry from which L_{acc} was determined is a potential problem because of variability. However, we do not feel that this has a significant effect on the line luminosity–L_{acc} correlations for the following reasons. First, simply finding such a tight correlation—among a sample of 19 stars—suggests that any changes in luminosity between the two (IR and UV) data sets on average were not greater than the breadth of the correlation. If variability introduced a truly large uncertainty in comparing the two data sets, one would expect any correlation to be degraded, not enhanced. Second, and most importantly, past quantitative estimates of intrinsic variability in both accretion luminosity and infrared line luminosity are not large enough to significantly affect the correlations. Typical veiling variations (and, correspondingly, variations in L_{acc}) are about 0.2–0.4 dex (Basri & Batalha 1990; Hartigan et al. 1991), similar to the error bars shown in Figure 4. Typical line emission variations are also not a significant factor; we observed five of the CTTS (AA Tau, BP Tau, DF Tau, DL Tau, and DR Tau) on two different nights, and the changes in line flux are either similar to or less than the measurement errors shown in Figure 4.

In order to verify that the line luminosities do indeed trace the accretion luminosity, we need to rule out other causes of these correlations. We compare the photometric magnitudes and extinctions to the accretion luminosities in Figure 5. None of these quantities can fully account for the tight correlations. The J magnitudes show little apparent

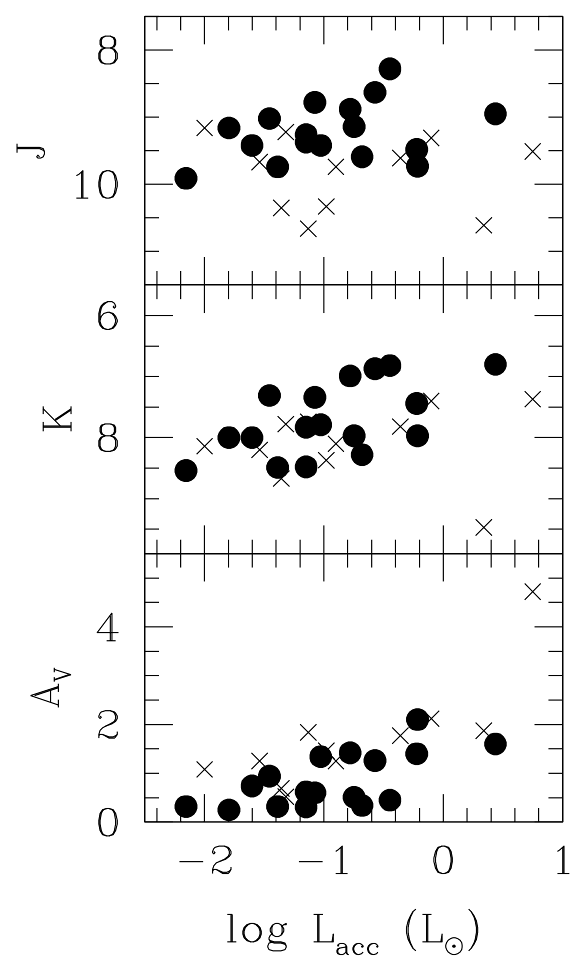

FIG. 5.—Correlations with the accretion luminosity. *Filled circles*, accretion rates from blue excess spectra; *crosses*, accretion rates from U-band photometry.

correlation with L_{acc}, as one would expect since it is primarily photospheric emission. The K magnitudes are somewhat correlated with L_{acc}, with considerable scatter. This is probably due to disk emission from accretion and/or stellar irradiation. However, the range of K-band brightnesses over the range of accretion rates is only about a factor of 6—much less than the factor of 100 range in line fluxes. Finally, the extinctions (at V) also show a slight correlation with L_{acc}, but the corresponding extinctions at J and K are much smaller (by factors of 0.3 and 0.1, respectively), and hence any effect on the line luminosity correlations would be trivial.

4. APPLICATION TO HEAVILY EXTINCTED SOURCES

4.1. *Comparison of Taurus and Ophiuchus Class II Sources*

As mentioned above, the standard method of determining disk mass accretion rates in highly reddened stars is inapplicable since the blue excess cannot be measured. In these cases, we can apply our infrared line luminosity calibration to sources with observed line luminosities to derive estimates of their accretion luminosities. We employ Brγ since it is least affected by extinction. First, we would like to calculate accretion luminosities for the highly extincted Class II objects (CTTS) in the ρ Ophiuchi star formation region, so we can compare to the Taurus CTTS. Greene & Lada (1996, hereafter GL) published near-infrared spectra of a large sample of young stellar objects in Ophiuchus; they detected Brγ emission in 10 Class II sources. Using their published line luminosities and equation (2), we obtain accretion luminosities for these objects (see Table 3). These are the first direct determinations of the accretion luminosity for CTTS in ρ Oph. Figure 6 compares the distribution of L_{acc} in ρ Oph to the GHBC sample in Taurus. The distributions are strikingly similar, and both peak at $L_{acc} \sim 0.1\ L_{\odot}$. Those CTTS in Ophiuchus with the lowest accretion luminosities are probably underrepresented here because of the detection limits of GL (see the following subsection). However, these results suggest that there are no gross differences in disk accretion between the two star formation regions.

4.2. *The Accretion Luminosity in Class I Sources*

Most previous work on Class I objects has relied on the assumption that the total luminosity is dominated by the accretion luminosity. This may be an overestimate if disk accretion rates are similar in Class I sources to CTTS, since the average CTTS accretion luminosity is only $\sim$10% of the total luminosity. If the accretion luminosity is indeed less than the total luminosity in embedded stars, then the luminosity problem discussed in the introduction becomes even worse.

TABLE 3

OPHIUCHUS CLASS II SOURCES

Object	log $L_{Br\gamma}/L_{\odot}$	log $L_{acc}/L_{\odot}$
SR 24N	−4.1	−0.74
DoAr 25	−4.6	−1.34
SR 22	−4.6	−1.34
SR 24S	−3.2	0.34
GY 93	−4.5	−1.22
VSS 27	−4.2	−0.86
VSSG 27	−4.2	−0.86
GSS 39	−4.0	−0.62
EL 24	−3.2	0.34
WL 18	−3.8	−0.38

NOTE.—Brγ line luminosities from GL.

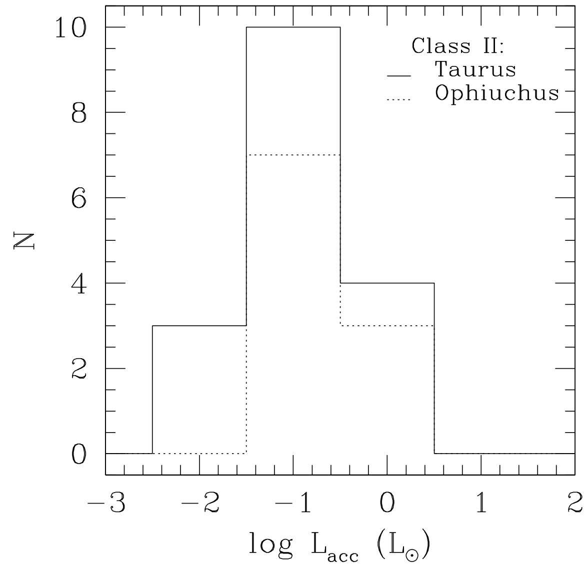

FIG. 6.—Distribution of accretion luminosities for Class II sources in Taurus (*solid line*) and Ophiuchus (*dotted line*).

The near-infrared spectra of GL include six Class I objects in Taurus-Auriga and 20 in ρ Ophiuchi with detected Brγ emission; we list those objects with available bolometric luminosities in Table 4. We note that three of the Ophiuchus sources have measurements of L_{bol} based on infrared fluxes only out to 20 μm or less (Wilking, Lada, & Young 1989); this clearly underestimates the total luminosity since the spectral energy distributions of most Class I sources peak at 60 μm or more. For this reason, we do not consider these sources in the subsequent figures and analysis.

We emphasize that there is considerable uncertainty in the Class I line luminosities because of the large extinction. Typical values for deeply embedded objects, $A_V \sim 20$–30, have a significant effect even at Brγ ($A_K \sim 2$–3). GL did not specify the extinctions and continuum fluxes they used to convert their observed line equivalent widths to line luminosities. We attempted to estimate their extinctions by using their equivalent widths and J- and K-band photometry from KH to compute line luminosities and then find the values of the extinction that reproduce GL's reported line ratios. From this we determined $A_V \sim 5$–15, less than expected for typical embedded stars. Hence, the accretion luminosities we derived from the Greene & Lada Brγ luminosities are probably lower limits.

The primary difficulty in estimating extinctions to embedded stars lies in disentangling the effects of absorption and scattering of the central star + disk emission by the infalling envelope. In the near-infrared, scattered light is the dominant component of the observed flux and can cause inferred extinctions to be too large. To circumvent somewhat the problem with the extinction, we attempted to estimate line luminosities using the GL equivalent widths and the "intrinsic" stellar K magnitudes ("K_0"), as determined for Taurus-Auriga embedded objects by Kenyon et al. (1993b, hereafter KWGH) from the bolometric luminosity of the object. Assuming each source is near the birth line in the HR diagram (Stahler 1983, 1988; Myers et al.

TABLE 4

CLASS I SOURCES

Object	log $L/L_{\odot}$	log $L_{acc}/L_{\odot}$ [a]	log $L_{acc}/L_{\odot}$ [b]	$K - K_0$
Taurus-Auriga				
04361+2547......	0.46	−1.10	−0.24	4.1
04016+2610......	0.57	−1.46	−0.48	3.2
04239+2436......	0.09	−0.62	0.065	2.7
GV Tau B	0.77	−1.34	−0.016	3.9
04489+3042......	−0.53	−1.70	−1.66	1.4
Haro 6-13	0.12	−0.74	−1.32	0.5
ρ Ophiuchi				
YLW 10B.........	0.26	−0.86	−0.57	3.3
WL 12	0.69	−1.10	−0.17	4.1
IRS 54	1.08	−1.34	0.51	5.7
WL 2.............	0.13	−0.86	−0.74	5.0
EL 29	1.68	1.18	1.25	3.8
WL 16	1.34	0.58	0.95	3.4
IRS 51	0.15	0.46	−0.83	1.5
GSS 26...........	−0.15[c]	−0.02	−0.57	1.3
WL 6.............	0.38[c]	−0.02	−0.37	3.2
WL 17	−0.49[c]	−0.50	−0.89	1.5

NOTE.—Bolometric luminosities from Kenyon et al. 1993a (Taurus sample) and Greene & Meyer 1995 and Wilking et al. 1989 (ρ Oph sample).

[a] Accretion luminosities derived from GL line luminosities.

[b] Accretion luminosities for Taurus sources derived using $K - K_0$ extinctions as in KWGH. Accretion luminosities for ρ Oph sources derived using $K - K_0$ extinctions calculated using the same method as KWGH, with K magnitudes from Barsony et al. 1997.

[c] Bolometric luminosities highly uncertain, based on infrared fluxes only out to 20 μm or less.

1987; Hartmann, Cassen, & Kenyon 1997), one can then determine an approximate effective temperature and then estimate the intrinsic J magnitude from an appropriate bolometric correction (see Gomez et al. 1992; KH). Then, assuming typical TTS colors, one can finally obtain the intrinsic K magnitude. We calculated K_0 for the ρ Oph sources using this technique and used the values quoted in KWGH for the Taurus-Auriga sources. The difference between the observed and intrinsic magnitudes, $K - K_0$, should then approximate the total effective extinction at K, combining the effects of scattered light and direct absorption. Typical values are $K - K_0 \sim 3$, much more consistent with that expected for embedded sources than the typical GL results of $\sim$0.5–1.5 (see Table 4).

As a consistency check, we also tried to estimate a correction factor, C_K, which measures the total loss of flux from the central star + disk owing to intervening material by using the infrared veiling of photospheric features (assuming that the veiling is due to the envelope). We can first do this using the observed K magnitudes and assuming an intrinsic K using typical values for an M0 TTS (estimates of spectral types from bolometric luminosities and an assumed age of 10^5 yr give spectral types of late-K and early-M for most of the Taurus embedded sources; KWGH). The total observed flux should be a combination of extincted and scattered central source light, $F_{*,e+s}$, plus additional flux from reprocessed radiation by the envelope, F_{ex} (Calvet, Hartmann, & Strom 1997). This can be expressed in terms of the veiling, defined by $r = F_{ex}/F_{*,e+s}$:

$$F_{obs} = (r + 1)F_{*,e+s} . \quad (3)$$

The correction factor we require is just the ratio of the observed flux from the central source to the intrinsic flux:

$$C = \frac{F_{*,e+s}}{F_*} . \quad (4)$$

With these two equations, we can obtain the correction factor if we know the veiling. Converting to magnitudes at K, we get

$$C_K = K - K_* + 2.5 \log (r_K + 1) , \quad (5)$$

where K_* is the intrinsic magnitude of the central source. For a typical TTS in Taurus of spectral type M0, $K_* \sim 8$. We estimated the veiling at K, r_K, from the CO absorption band indices of Casali & Eiroa (1996). Unfortunately, we can calculate C_K for only two sources, 04016+2610 and Haro 6-13, because of a lack of veiling measurements. The results, $C_K = 3.4, 0.6$, compare very favorably with $K - K_0 = 3.2, 0.5$ (respectively).

Using the Brγ line luminosities and equation (2), we then get accretion luminosities for the objects listed in Table 4; these are plotted versus L_{bol} in Figure 7. Two values of L_{acc} are shown for each object: one from the GL line luminosities and one using the $K - K_0$ extinctions. Figure 7 shows that the total luminosities are on average an order of magnitude greater than the derived accretion luminosities, consistent with typical values in TTS. However, there is a large spread between the two different determinations of L_{acc} for many objects, which indicates the level of uncertainty in the extinction toward embedded objects. The extinction is the limiting factor to determining accurate accretion luminosities, even with the Brγ calibration. Nevertheless, we obtain similar results for Class I objects in two quite different star formation regions, which strongly argues for $L_{acc} < L_{bol}$, despite the uncertainties.

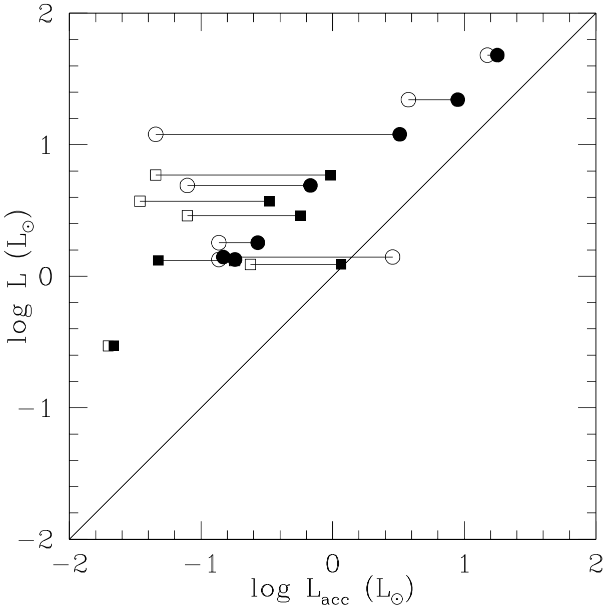

FIG. 7.—Comparison of the total and accretion luminosities for Class I sources. *Circles*, ρ Oph sources; *squares*, Taurus sources. Open points correspond to line luminosities from GL; filled points correspond to line luminosities using the effective extinction values $K - K_0$ as in KWGH.

As a final check, a maximum correction factor, C_K, can be determined assuming $L_{acc} = L_{bol}$. The expected Brγ line luminosity can be determined from L_{acc} by inverting equation (2). From the observed K magnitudes and Brγ equivalent widths, we can then estimate the correction factor as an equivalent extinction that yields the expected line luminosity. The resultant values of C_K from this method range from 3 to 6 mag. In many if not all cases, the values seem implausibly large. As a consistency check, we can substitute into equation (5) and solve for the intrinsic magnitude, K_*. For the two sources for which we can get the veiling at K, we derive K_* of about 6, rather than 8 (as above); if the spectral types are K or later, this would put the stars far above the birth line in the HR diagram (and yield values for L_{bol} much higher than what is observed). We also note that another source, 04489+3042, has been observed with NICMOS (Chen, Hartmann, & Calvet 1998), and the central object appears as a point source in H, K, and possibly J. This seems to favor the low $K - K_0$ value for this object (as well as the extinction used by GL, since there is little difference in Fig. 7) as the true extinction, rather than the large C_K we estimated.

5. DISCUSSION

5.1. *Magnetospheric Accretion*

Observed high-resolution line profiles of Paβ and Brγ in CTTS (Folha, Emerson, & Calvet 1997) and Brγ in embedded objects (Najita, Carr, & Tokunaga 1996) are qualitatively consistent with our magnetospheric model profiles (Muzerolle et al. 1998a). The model line fluxes, shown in Figure 3, also are in general agreement with our observations. However, the models do not predict that there should be such a tight correlation of the line fluxes with the accretion rate. Other parameters, most importantly magnetosphere size and temperature, also have a significant effect on the line flux. Thus, the physical basis for the correlations is not clear—it is possible that the temperature and size of the magnetosphere also depend on the accretion rate in such a way as to enhance the correlation. We also note that these models are appropriate only for typical TTS masses and radii, which may not apply for some of the Class I sources. Further modeling must be done to explore these problems in detail.

5.2. *Disk Accretion and the Central Star in Class I Objects*

Our results suggest that the accretion luminosity in many Class I objects is on the order of that for the (presumably older) classical T Tauri stars. This is in conflict with typical steady accretion models, in which the star is built up from disk accretion at the same rate as the infall of the protostellar envelope.

Because we do not understand the physics of our L_{acc}-Brγ correlation well, and because our calibration sample is restricted to roughly a fixed mass, one could argue that our estimates are misleading since they do not apply to the typical Class I stellar mass. However, Figure 7 indicates that most of the central luminosity comes from the star in most cases; then the Taurus luminosity distribution similarity between Class I and Class II objects suggests that the two groups represent a similar population (see KH). We then obtain a typical protostellar luminosity of $\sim 1\ L_\odot$, which corresponds to a stellar mass (on the birth line) of ~ 0.3–$0.5\ M_\odot$, which is typical of Class II objects (and of our calibration sample). In addition, Kenyon et al. (1998) found optical spectral types for several Taurus Class I sources, all of which were M type, roughly consistent with the median spectral type K7–M0 of the CTTS in our calibration sample. However, we need to pursue the L_{acc}-Brγ correlation for lower mass stars to help support these results.

Another reason why we might derive a biased result is that at high accretion rates, the magnetosphere could be crushed by the disk, eliminating the line emission. Thus, we can apply our method only to low-L_{acc} objects. However, the method does apply to a large fraction of the GL ρ Oph sample, in which about 50% each of the Class I, flat spectrum, and Class II sources exhibit Brγ emission; no Class III sources show any emission. These data indicate that the Brγ emission characteristics are not significantly different among the different classes of objects, as long as the sources are actively accreting. Moreover, the lack of detectable Brγ emission is not necessarily due to magnetospheric crushing; at low accretion rates, the emission is hard to detect. After smoothing our data to their resolution ($R \sim 500$ for about 75% of the ρ Oph sample, $R \sim 700$ for the rest), Brγ emission with equivalent widths of less than 1.5–2 Å cannot be detected. This includes about half of our calibration sample and corresponds to most stars with less than average accretion luminosities. Of the three Taurus sources without detected line emission, two have smaller than average bolometric luminosities, and so are likely to have less than average accretion luminosities. The other, L1551 IRS 5 (a suspected embedded FU Ori object), has a large bolometric luminosity ($L_{bol} = 22\ L_\odot$), and may be a case of a crushed magnetosphere. Thus, we think that our calibration can provide typical results for Class I objects.

If typical T Tauri disk accretion rates ($10^{-8}\ M_\odot\ yr^{-1}$) also apply for the younger Class I sources, there is not enough time to accrete to the final stellar mass (given typical TTS ages of a few times 10^6 yr). Additionally, the typical envelope infall rate is then up to 2 orders of magnitude larger than the disk accretion rate; material is rapidly piling up in the disk, and gravitational instabilities are likely

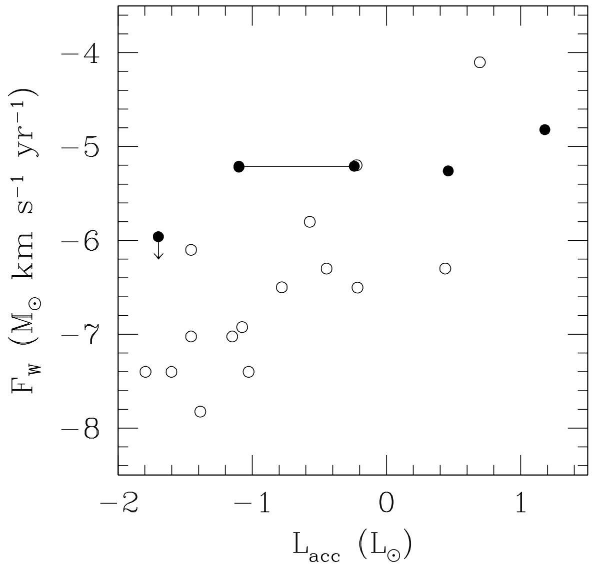

FIG. 8.—Wind momentum flux vs. accretion luminosity for CTTS (*open circles*) and Class I objects (*filled circles*). CTTS momentum flux from [O I] λ6300 high-velocity component; accretion luminosities from GHBC. Class I momentum flux from ^{12}CO(2–1) outflows (Bontemps et al. 1996); accretion luminosities from Brγ line luminosities (GL) (line indicates range including estimate from $K - K_0$ for one source, 04361+2547).

to occur. These two consequences strongly argue for episodic accretion events (i.e., FU Orionis or EX Orionis outbursts) at the Class I stage of evolution, in which the disk accretion rate is several orders of magnitude higher on very short (~100 yr) timescales. Most of the circumstellar material then accretes onto the star during these brief episodes, and perhaps in a very brief initial episode at the beginning of collapse (Henriksen, André, & Bontemps 1997).

5.3. *The Outflow Connection*

Class I sources also exhibit strong outflows. A comparison of accretion and outflow phenomena in Class I and Class II objects provides further insight into the evolution of these objects. We take a preliminary look in Figure 8, which shows the variation of the wind momentum flux as a function of accretion luminosity for both CTTS and Class I sources. Wind momentum fluxes for the CTTS are derived from the mass-loss rates and velocities determined by Hartigan et al. (1995) from the [O I] λ6300 line. For the Class I sources, we used the CO outflow momentum fluxes given in Bontemps et al. (1996) for the sources with published Brγ line luminosities.

Unfortunately, there are only a few sources with both CO momentum fluxes and Brγ line luminosities; thus, any result gleaned from Figure 8 is far from conclusive. Nevertheless, Figure 8 indicates that the Class I sources overlap CTTS in the level of wind momentum flux and its relation with the accretion luminosity. The Class I objects may have somewhat higher momentum fluxes; however, given the large dynamical timescales ($\gtrsim 10^4$ yr; Saraceno et al. 1996) of the CO outflows, the CO momentum flux may actually overestimate the present *wind* momentum flux, and so could have been generated by outbursts during this timescale.

6. CONCLUSIONS

We have found that the emission-line luminosities of Paβ and Brγ in CTTS highly correlate with the disk accretion rate/luminosity. Our calibration of the infrared emission-line luminosity tracer provides a powerful tool for determining L_{acc} in Class I and other highly reddened objects. We have applied this calibration to a small sample of Taurus and ρ Ophiuchi Class I sources with previously published Brγ measurements; the inferred accretion luminosities are in general less than the total source luminosities, contrary to previous assumptions. This result suggests that the time-averaged disk accretion rate is much smaller than the infall rate, supporting the notion that periodic FU Ori outbursts are necessary to deliver the bulk of the circumstellar material to the young star. However, we have emphasized that extinction, large even at K and complicated by envelope scattering in Class I objects, must be correctly accounted for when measuring Brγ line luminosities.

Last, we note that the infrared line calibration has a potentially wide range of applicability. The standard method of deriving accretion luminosities from the blue excess is invalid in many cases other than Class I objects. In any case where the extinction is so high that blue/UV fluxes cannot be determined accurately or cannot be determined at all (not necessarily Class I objects), this new method can be used. Also, CTTS more massive than ~1.5 $M_\odot$ have photospheres hot enough to effectively mask the accretion shock emission—measurements of the hot continuum excess are essentially impossible in these cases. Infrared line emission is observed in these intermediate-mass stars and should be able to trace the accretion luminosity, although further study is required in order to determine whether the stellar mass and related properties have an effect on the line/accretion luminosity calibration.

We thank Dick Joyce for assistance at KPNO, Erik Gullbring and Cesar Briceño for stimulating discussions, and Mike Meyer and Jim Emerson for sharing infrared observation expertise. We also acknowledge the referee, Claude Bertout, for useful comments. J. M. thanks Steve Strom and Suzan Edwards for encouragement and helpful discussions. This work was supported in part by NASA grant NAG 5-4282.

REFERENCES

Adams, F. C., Lada, C. J., & Shu, F. H. 1987, ApJ, 312, 788
Barsony, M., Kenyon, S. J., Lada, E. A., & Teuben, P. J. 1997, ApJS, 112, 109
Basri, G., & Batalha, C. 1990, ApJ, 363, 654
Basri, G., & Bertout, C. 1989, ApJ, 341, 340
Bertout, C., Basri, G., & Bouvier, J. 1988, ApJ, 330, 350
Bontemps, S., André, P., Terebey, S., & Cabrit, S. 1996, A&A, 311, 858
Calvet, N., & Gullbring, E. 1998, ApJ, in press
Calvet, N., & Hartmann, L. 1992, ApJ, 386, 239
Calvet, N., Hartmann, L., & Strom, S. 1997, ApJ, 481, 912
Casali, M. M., & Eiroa, C. 1996, A&A, 306, 427
Chen, H., Hartmann, L., & Calvet, N. 1998, in preparation
Edwards, S., Hartigan, P., Ghandour, L., & Andrulis, C. 1994, AJ, 108, 1056
Folha, D., Emerson, J., & Calvet, N. 1997, in IAU Symp. 182, Low Mass Star Formation—From Infall to Outflow (Poster Proceedings), ed. F. Malbet & A. Castets (Grenoble: Obs. Grenoble), 272
Gomez, M., Jones, B. F., Hartmann, L., Kenyon, S. J., Stauffer, J. R., Hewett, R., & Reid, I. N. 1992, AJ, 104, 762
Greene, T. P., & Lada, C. J. 1996, AJ, 112, 2184 (GL)
Greene, T. P., & Meyer, M. R. 1995, ApJ, 450, 233
Gullbring, E., Hartmann, L., Briceño, C., & Calvet, N. 1998, ApJ, 492, 323 (GHBC)
Hartigan, P., Edwards, S., & Ghandour, L. 1995, ApJ, 452, 736

Hartigan, P., Kenyon, S. J., Hartmann, L., Strom, S. E., Edwards, S., Welty, A., & Stauffer, J. 1991, ApJ, 382, 617
Hartmann, L., Calvet, N., Gullbring, E., & D'Alessio, P. 1998, ApJ, 495, 385 (HCGD)
Hartmann, L., Cassen, P., & Kenyon, S. J. 1997, ApJ, 475, 770
Hartmann, L., Hewett, R., & Calvet, N. 1994, ApJ, 426, 669
Henriksen, R., André, P., & Bontemps, S. 1997, A&A, 323, 549
Kenyon, S. J., Brown, D. I., Tout, C. A., & Berlind, P. 1998, AJ, 115, 2491
Kenyon, S. J., Calvet, N., & Hartmann, L. 1993a, ApJ, 414, 676
Kenyon, S. J., & Hartmann, L. 1987, ApJ, 323, 714
———. 1995, ApJS, 101, 117 (KH)
Kenyon, S. J., Hartmann, L., Strom, K., & Strom, S. 1990, AJ, 99, 869
Kenyon, S. J., Whitney, B. A., Gomez, M., & Hartmann, L. 1993b, ApJ, 414, 773 (KWGH)
Muzerolle, J., Calvet, N., & Hartmann, L. 1998a, ApJ, 492, 743
Muzerolle, J., Hartmann, L., & Calvet, N. 1998b, AJ, 116, 455
Myers, P. C., Fuller, G. A., Mathieu, R. D., Beichman, C. A., Benson, P. J., Schild, R. E., & Emerson, J. P. 1987, ApJ, 319, 340
Najita, J., Carr, J. S., & Tokunaga, A. T. 1996, ApJ, 456, 292
Saraceno, P., André, P., Ceccarelli, C., Griffin, M., & Molinari, S. 1996, A&A, 309, 827
Stahler, S. W. 1983, ApJ, 274, 822
———. 1988, ApJ, 332, 804
Valenti, J., Basri, G., & Johns, C. 1993, AJ, 106, 2024
Wilking, B. A., Lada, C. J., & Young, E. T. 1989, ApJ, 340, 823